HHS Public Access

Author manuscript

Anal Chem. Author manuscript; available in PMC 2021 July 15.

Published in final edited form as:

Anal Chem. 2020 May 05; 92(9): 6334–6340. doi:10.1021/acs.analchem.9b05194.

Mitigating the Effects of Electrode Biofouling-Induced Impedance for Improved Long-Term Electrochemical Measurements In Vivo

Blake T. Seaton,
Department of Chemistry and Biochemistry, University of Arizona, Tucson, Arizona, United States

Daniel F. Hill,
Department of Physiology, University of Arizona, Tucson, Arizona, United States

Stephen L. Cowen,
Department of Psychology and Evelyn F. McKnight Brain Institute, University of Arizona, Tucson, Arizona, United States

Michael L. Heien
Department of Chemistry and Biochemistry, University of Arizona, Tucson, Arizona, United States

Abstract

Biofouling is a prevalent issue in studies that involve prolonged implantation of electrochemical probes in the brain. In long-term fast-scan cyclic voltammetry (FSCV) studies, biofouling manifests as a shift in the peak oxidative potential of the background signal that worsens over days to weeks, diminishing sensitivity and selectivity to neurotransmitters such as dopamine. Using open circuit potential (OCP) measurements, scanning electron microscopy/energy-dispersive X-ray spectroscopy (SEM/EDX), and electrochemical impedance spectroscopy (EIS), we examined the biofouling-induced events that occur due to electrode implantation. We determined that the FSCV background signal shift results from cathodic polarization of the Ag/AgCl-wire reference electrode and increased electrochemical impedance of both the Ag/AgCl-wire reference electrode and carbon-fiber working electrode. These events are likely caused collectively by immune response-induced electrode encapsulation. A headstage utilizing a three-electrode configuration, designed to compensate for the impedance component of biofouling, reduced the FSCV background signal shift in vivo and preserved dopamine sensitivity at artificially increased impedance levels in vitro. In conjunction with a stable reference electrode, this three-electrode configuration will be critical in achieving reliable neurotransmitter detection for the duration of long-term FSCV studies.

Corresponding Author Michael L. Heien, Phone: 520-621-6293; mheien@arizona.edu; Fax: 520-621-8407.

Author Contributions

B.T.S. designed experiments, performed surgeries, performed experiments, analyzed data, generated figures, and wrote the manuscript. D.F.H. performed surgeries and reviewed the manuscript. S.L.C. reviewed the manuscript. M.L.H. proposed the study and reviewed the manuscript.

Supporting Information

The Supporting Information is available free of charge at https://pubs.acs.org/doi/10.1021/acs.analchem.9b05194.

Photo and circuit schematic of three-electrode headstage (PDF)

The authors declare no competing financial interest.

Graphical Abstract

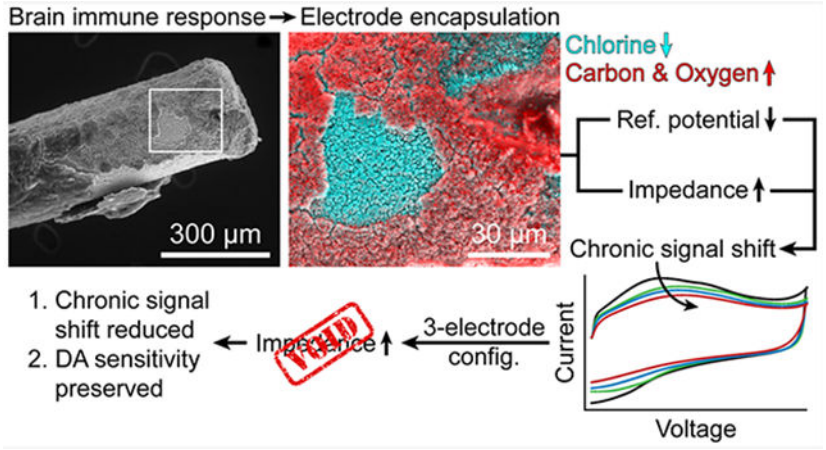

Alterations in long-term dopaminergic signaling affect many physiological and behavioral systems and are implicated in the etiology of neurodegenerative diseases, chronic pain, and mental disorders.[1-5] Fast-scan cyclic voltammetry (FSCV) is an electrochemical technique that allows dopaminergic release to be investigated in real time.[6-10] FSCV measurement requires the subtraction of background current, necessitating a stable background signal over the course of the study for reliable detection of dopamine. Long-term FSCV studies thus present a challenge, as the chronic (i.e., permanent) implantation of electrodes in the brain elicits a cascade of immune responses (e.g., gliosis) that target the electrodes and degrade voltammetric performance, an effect generally referred to as biofouling.[11-18] In FSCV, biofouling manifests as a shift in the peak oxidative potential of the background signal ($E_{P,Bkg}$) that begins days after implantation and worsens over the course of weeks. Since the potentials of the resultant cyclic voltammogram after background subtraction serve as a chemical “fingerprint” for detected species, the $E_{P,Bkg}$ shift obscures analyte identification and reduces sensitivity.[10]

Several strategies have been employed to attempt to return $E_{P,Bkg}$ to its original potential after prolonged electrode implantation in the brain. Commonly, the applied potential waveform (−0.4 to 1.3 to −0.4 V vs Ag/AgCl) is purposefully offset by +200 mV (i.e., −0.2 to 1.5 to −0.2 V vs Ag/AgCl),[19-21] a strategy that can appear to be effective because $E_{P,Bkg}$ often shifts to approximately 200 mV from its original value. However, this is not an ideal solution because the time scale and magnitude of the $E_{P,Bkg}$ shift are variable across animals and the accuracy of the applied potential waveform is compromised. The potential offset strategy is employed as a universal solution to a variable problem. Another strategy involves the acute implantation of electrodes through chronically implanted guide cannulae for each experiment.[22-24] This is not an ideal solution, as it is best to implant all electrodes on the day of surgery to avoid additional brain intrusion after recovery and to minimize the risk of infection. Other strategies for combating the effects of biofouling, such as chemical modifications of the electrode surfaces, have yielded varying degrees of success.[25-29]

Herein, we identify two events that cause the $E_{P,Bkg}$ shift in long-term FSCV: (1) cathodic polarization of the Ag/AgCl-wire reference electrode and (2) increased electrochemical impedance of both the carbon-fiber working electrode and Ag/AgCl-wire reference electrode. Both events are likely caused by immune response-induced encapsulation of the electrodes. It was shown by Clark et al. that the immune response to chronically implanted carbon-fiber electrodes subsides after several months in the brain,[21] though the long-term effects that the initial immune response has on both the carbon-fiber working electrode and Ag/AgCl-wire reference electrode remained unclear. We thus sought to investigate the biofouling-induced changes that occur at both electrodes at time points closer to the day of implantation.

FSCV is conventionally performed in a two-electrode configuration (carbon-fiber working electrode, Ag/AgCl-wire reference electrode) due to the small currents passed at microelectrodes and negligible electrochemical impedance levels in the brain upon implantation. Since the encapsulation of implanted electrodes is not a rapid process, the two-electrode configuration is suitable for acute (i.e., one-day) FSCV studies. However, the increase in electrochemical impedance that occurs during prolonged brain implantation makes the two-electrode configuration unsuitable for long-term studies. We demonstrate that a three-electrode configuration, utilizing a Pt-wire counter electrode, compensates for increased electrochemical impedance and reduces the $E_{P,Bkg}$ shift in vivo. We also demonstrate the ability of the three-electrode configuration to preserve dopamine sensitivity at artificially increased impedance levels in vitro.

While the three-electrode configuration mitigates the impedance component of biofouling, the cathodic polarization of the Ag/AgCl-wire reference electrode remains an issue. Nafion-coating the reference electrode has been shown to delay the onset of polarization,[25] but a permanent solution is yet to be developed. Further, the toxicity of silver in the brain warrants the use of a more biocompatible reference electrode material. A stable, biocompatible reference electrode in conjunction with the three-electrode configuration demonstrated herein is the ideal combination for long-term FSCV.

MATERIALS AND METHODS

Chemicals.

Tris HCl (CAS 1185–53–1), Tris base (CAS 77–86–1), magnesium chloride hexahydrate (CAS 7791–18–6), calcium chloride dihydrate (CAS 10035–04–8), and dopamine hydrochloride (CAS 62–31–7) were purchased from Sigma-Aldrich (St. Louis, MO). Sodium sulfate anhydrous (CAS 7757–82–6) and sodium phosphate monobasic monohydrate (CAS 10049–21–5) were purchased from Mallinckrodt Baker (Phillipsburg, NJ). Sodium chloride (CAS 7647–14–5), potassium chloride (CAS 7447–40–7), hydrochloric acid (CAS 7647–01–0), and isopropanol (CAS 67–63–0) were purchased from EMD Millipore (Burlington, MA). Perchloric acid (CAS 7601–90–3) was purchased from Avantor Performance Materials (Center Valley, PA). Dopamine stock was prepared by dissolving dopamine hydrochloride in 0.1 M $HClO_4$. Artificial cerebrospinal fluid (aCSF) was composed of 15 mM Tris HCl, 10 mM Tris base, 126 mM NaCl, 2.5 mM KCl, 1.2 mM $NaH_2PO_4{\cdot}H_2O$, 2 mM Na_2SO_4 anh., 2.4 mM $CaCl_2{\cdot}2H_2O$, and 1.2 mM $MgCl_2{\cdot}6H_2O$.

Before addition of $CaCl_2$ and $MgCl_2$, the aCSF was adjusted to pH 7.40 with HCl. Water was purified to 18.2 MΩ·cm with a Milli-Q Gradient A10 water purification system (EMD Millipore, Burlington, MA).

Electrode Fabrication.

Carbon-fiber electrodes were fabricated as previously described, with minor modifications.[21] A single 7.1 μm-diameter carbon fiber (AS4 12K, Hexcel, Stamford, CT) was inserted into a 15 mm-long fused silica capillary (20-μm ID, 90-μm OD, 1068150381, Polymicro, Phoenix, AZ) in isopropanol. One end of the capillary was sealed with Devcon two-ton epoxy (14310, ITW Performance Polymers, Danvers, MA), leaving a small length of exposed carbon fiber. On the opposite end, the carbon fiber was connected to a gold-plated beryllium–copper–nickel pin (SPC15510, Multicomp by Newark, Chicago, IL) with alcohol-based graphite conductive adhesive (42465, Alfa Aesar, Ward Hill, MA), followed by epoxy. The exposed carbon fiber was cut to a length of 100 μm with a scalpel under a Micromaster brightfield microscope (12–561B, Fisher Scientific, Hampton, NH). Ag/AgCl-wire reference electrodes were prepared by soaking 0.25 mm-diameter silver wire (265578, Sigma-Aldrich, St. Louis, MO) in 8.25% sodium hypochlorite (The Clorox Company, Oakland, CA) for 24 h. Counter electrodes were 0.25 mm-diameter platinum wire (349402, Sigma-Aldrich, St. Louis, MO).

Animals and Surgery.

Male Sprague–Dawley rats (3–4 months, 373–510 g, Envigo, Huntingdon, Cambridgeshire, U.K.) were housed two per cage on a 12 h light/dark cycle with food and water provided ad libitum. On the day of surgery, rats were anesthetized with 3.5% isoflurane gas and an oxygen flow rate of 1.5 L/min. Before surgery, gentamicin (8 mg/kg, SC) and ketoprofen (5 mg/kg, SC) were administered and ophthalmic ointment (Puralube, Dechra, Overland Park, KS) was applied to the eyes. During the surgical procedure and all experiments, isoflurane was kept between 0.7 and 2% and oxygen was kept at 1.5 L/min. The rat's body temperature was maintained with a water-circulating heating pad (T/Pump, Stryker, Portage, MI). A carbon-fiber electrode was lowered into the nucleus accumbens (AP: 1.5 mm, ML: 1.3 mm, DV: −6.7 mm relative to bregma). A 22-gauge PEEK guide cannula (C313G/PK/SPC, Plastics One, Roanoke, VA) was lowered 3 mm into the ipsilateral hemisphere, posterior to the carbon-fiber electrode. When not in use, the guide cannula was kept closed with a 0.33 mm diameter nylon obturator (C313DCN/SPC, Plastics One, Roanoke, VA). A Ag/AgCl-wire reference electrode and Pt-wire counter electrode were each lowered 4 mm into the contralateral hemisphere, with the Pt-wire electrode posterior to the Ag/AgCl-wire electrode. Implants were secured with dental acrylic (44115, Yates Motloid, Chicago, IL) bonded to skull-anchored stainless-steel screws with C&B Metabond (S380, Parkell, Edgewood, NY). Gentamicin (8 mg/kg, SC) was administered 24 h postsurgery and ketoprofen (5 mg/kg, SC) was administered 24 and 48 h postsurgery. Triple antibiotic topical ointment (Medi-First, Fort Myers, FL) was applied to the surgical area immediately postsurgery and once per day thereafter for a maximum of 4 days postsurgery. Upon completion of the three-week study, the chronically implanted Ag/AgCl-wire reference electrode was explanted for SEM/EDX analysis. All experiments were approved by the University of Arizona Institutional Animal Care and Use Committee.

Fast-Scan Cyclic Voltammetry (FSCV).

In all in vivo and in vitro FSCV experiments, a carbon-fiber working electrode, Ag/AgCl-wire reference electrode, and Pt-wire counter electrode (when using the three-electrode configuration) were utilized with custom-built hardware and LabVIEW software. To condition the carbon-fiber electrode before recordings, a triangular potential waveform (−0.4 to 1.3 to −0.4 V vs Ag/AgCl wire) was applied at 400 V/s and 60 Hz until the background signal stabilized. The waveform frequency was then lowered to 10 Hz and the signal again allowed to stabilize. Background signal stabilization was defined as a current drift of less than 0.5 nA/min at 0.6 V and typically required 20–30 min of 60 Hz cycling followed by 10–15 min of 10 Hz cycling. All background signal traces are presented as raw, unfiltered data. A fourth-order Butterworth low-pass filter (f_c = 1.66 kHz) was applied to all background signals before $E_{P,Bkg}$ determination.

Dopamine Calibration Curves.

Dopamine calibration curves were collected in vitro by performing FSCV in a 20 mL vial of aCSF until background signal stabilization (vide supra), then injecting a known concentration of dopamine under constant magnetic stirring. The steady-state current reached after dopamine injection was recorded. After each recording, all electrodes were rinsed with nanopure water and the procedure was repeated in a new vial.

Open Circuit Potential (OCP) and Electrochemical Impedance Spectroscopy (EIS).

OCP and EIS measurements were made using a Reference 600 potentiostat (Gamry Instruments, Warminster, PA). OCP recordings were performed in vivo with the chronically (i.e., permanently) implanted Ag/AgCl wire as the working electrode and a validated Ag/AgCl wire inserted through the guide cannula as the reference electrode. Ag/AgCl-wire reference electrodes were defined as “validated” if their potential fell within 46–50 mV vs a commercial Ag/AgCl reference electrode (1 M KCl, CHI111, CH Instruments, Austin, TX) in vitro (aCSF). This target potential range was determined with 15 Ag/AgCl-wire reference electrodes and represents the mean ± 3 SD (48 ± 2 mV). EIS was performed in a three-electrode configuration with either the chronically implanted Ag/AgCl wire or carbon fiber as the working electrode, a validated Ag/AgCl wire inserted through the guide cannula as the reference electrode, and the chronically implanted Pt wire as the counter electrode. A 10 mV (rms) perturbation waveform centered at 0 V (vs OCP) was applied at frequencies from 1 MHz to 1 Hz at 10 points per decade.

Scanning Electron Microscopy/Energy-Dispersive X-ray Spectroscopy (SEM/EDX).

Scanning electron micrographs were collected under high vacuum with a 3 nm spot size and 30 kV excitation voltage on an Inspect S50 scanning electron microscope (FEI Company, Hillsboro, OR). EDX data were collected and quantified using a NORAN System Six X-ray microanalysis system (Thermo Fisher Scientific, Waltham, MA).

RESULTS AND DISCUSSION

To investigate the effect of biofouling on the peak oxidative potential of the FSCV background signal ($E_{P,Bkg}$), a carbon-fiber working electrode and Ag/AgCl-wire reference

electrode were chronically (i.e., permanently) implanted in the rat brain and the FSCV background signal was recorded weekly. Using a conventional two-electrode configuration, $E_{P,Bkg}$ shifted progressively each week after implantation (Figure 1A). The $E_{P,Bkg}$ shift became significant after 1 week of implantation (Figure 1B). Commonly, a +200 mV offset is applied to compensate for this shift.[19-21] This strategy can appear to be an effective solution but its universal use is unwarranted, considering the variability in time scale and magnitude of the $E_{P,Bkg}$ shift across animals and the resultant inaccuracy in the applied waveform. Herein, we observed a $E_{P,Bkg}$ shift of 164 ± 20 mV (mean ± SEM, $n = 4$ rats) vs chronic Ag/AgCl wire after 3 weeks of implantation. The variability in the shift (95% CI [85–242 mV] vs chronic Ag/AgCl wire, 3 weeks post-implantation) provides further evidence that the +200 mV offset strategy is not an ideal solution.

Scanning electron microscopy (SEM) was used to examine the Ag/AgCl-wire reference electrodes before and after brain implantation. Figure 2 illustrates the changes that occurred on the surfaces of these electrodes after 3 weeks of implantation. The granular, homogeneous topography of the Ag/AgCl-wire electrodes was no longer visible post-implantation due to an encapsulating sheath of material likely induced by the immune response to electrode implantation in the brain.

To investigate these changes on a chemical level, energy-dispersive X-ray spectroscopy (EDX) was employed. Before implantation, EDX of the Ag/AgCl-wire reference electrode surfaces showed strong peaks for silver and chlorine (Figure 3A, black). After 3 weeks of implantation, EDX revealed a significant decrease in chlorine and a significant increase in carbon and oxygen on the Ag/AgCl-wire reference electrode surfaces (two-tailed paired t test, Figure 3B). A small amount of sulfur was also detected post-implantation, though this change from none detected preimplantation was not significant ($p > 0.05$).

There are previous reports of decreased surface chlorine on Ag/AgCl-wire reference electrodes after prolonged in vivo implantation.[25,30] The decrease is often attributed to gradual loss of the chloride layer over time, or “dechlorination”.[10,30] Herein, dechlorination was accompanied by the formation of an organic sheath around the electrode, likely induced by the immune response to implantation in the brain. Figure 4 shows the encapsulation of a Ag/AgCl-wire reference electrode after 3 weeks of implantation. Due to small voids in the encapsulating sheath, what remained of the granular chloride layer could be seen underneath. Using EDX spectral mapping, the uncovered area was confirmed to be chlorine and the surrounding material confirmed as organic (Figure 4B).

The potential of a Ag/AgCl reference electrode is stable when a chloride equilibrium exists between the electrode surface and the surrounding medium (i.e., when the chloride ion activity is constant). This is explained by the Nernst equation (eq 1), which relates the potential of a Ag/AgCl electrode to chloride ion activity. Specifically, as chloride ion activity decreases, the electrode polarizes to more anodic (i.e., positive) potentials.

$$E = E^0 - \frac{RT}{F} \ln(a_{Cl^-}) \quad (1)$$

In eq 1, E is the potential of the Ag/AgCl electrode, E^0 is the standard potential of the Ag/AgCl electrode (0.222 V vs SHE[31]), R is the ideal gas constant, T is temperature, F is Faraday's constant, and a_{Cl^-} is chloride ion activity. When the chloride equilibrium is disrupted in vivo (e.g., by electrode encapsulation and dechlorination), chloride ion activity presumably decreases. According to eq 1, this should result in anodic polarization of the Ag/AgCl-wire reference electrode over time in vivo. To investigate this, the open circuit potential of the chronically implanted Ag/AgCl-wire reference electrode was measured vs validated Ag/AgCl wire (vide supra) acutely implanted through a guide cannula each week. The chronically implanted Ag/AgCl-wire reference electrode did polarize over the course of 3 weeks, but in the cathodic direction (Figure 5A). The highly reproducible potentials of our Ag/AgCl-wire reference electrodes (Figure 5B) allowed for the polarization to be attributed solely to the chronically implanted Ag/AgCl-wire reference electrode. We observed a chronic polarization of −123 ± 30 mV (mean ± SEM, $n = 4$ rats) vs validated Ag/AgCl wire, 3 weeks post-implantation.

The cathodic polarization of Ag/AgCl-wire reference electrodes in vivo is further illustrated in Figure 6, which shows the experimentally determined potentials of our Ag/AgCl-wire reference electrodes in vitro and in vivo, compared to literature values for commercial Ag/AgCl reference electrode potentials.

Cathodic polarization of chronically implanted Ag/AgCl-wire reference electrodes has been reported previously.[30,33] Interestingly, the direction of polarization observed in those studies and herein contradicts that predicted by eq 1, suggesting that loss of chloride ion activity is not the dominant factor in chronic Ag/AgCl-wire reference electrode polarization in vivo. The chemical mechanism behind this phenomenon is currently under investigation.

We hypothesized that cathodic polarization of the chronically implanted Ag/AgCl-wire reference electrode was not the sole contributor to the $E_{P,Bkg}$ shift, as the magnitude of the $E_{P,Bkg}$ shift was larger than that of the reference electrode polarization at all time points of the study. There are numerous reports of increased electrochemical impedance of chronically implanted probes due to the immune response of the brain.[34-38] Electrochemical impedance spectroscopy (EIS) was employed in vivo in a three-electrode configuration to allow for evaluation of the impedance profiles of the chronically implanted Ag/AgCl-wire reference electrode and carbon-fiber working electrode independently (Figure 7). Two-way repeated measures ANOVA showed a significant difference in impedance for both electrodes when comparing time post-implantation ($F_{3,366} = 1088$ (reference electrode), 1137 (working electrode), $p < 0.0001$ (both electrodes), $n = 3$ rats). Bonferroni posthoc tests showed that the Ag/AgCl-wire reference electrode and carbon-fiber working electrode experienced significantly increased impedance levels at frequencies below 100 and 30 Hz, respectively ($p < 0.05$). Elevated electrochemical impedance in the mid- to low-frequency range is associated with charge-transfer resistance.[39] Increased charge-transfer resistance of chronically implanted Ag/AgCl-wire reference electrodes has been reported previously by Wang et al.[33]

The widely accepted two-electrode FSCV configuration (carbon-fiber working electrode, Ag/AgCl-wire reference electrode) is valid for acute (i.e., one-day) studies because the

currents passed at microelectrodes are small and electrochemical impedance levels are negligible in the brain upon implantation. However, the increase in electrochemical impedance that occurs during prolonged brain implantation makes the two-electrode configuration unsuitable for long-term studies. To compensate for the impedance component of the $E_{P,Bkg}$ shift, a headstage utilizing a three-electrode configuration was designed and fabricated. This configuration uses a platinum counter electrode, which senses the potential between the working and reference electrodes and alters its current supply to the working electrode, guaranteeing accuracy in the applied potential, even at increased impedance levels. The three-electrode headstage and circuit schematic are shown in Figure S1.

Based on previous work by Roberts et al., Randles equivalent circuits were constructed and used to artificially increase electrochemical impedance in vitro (aCSF).[40] As the charge-transfer resistance value of the circuit was increased, the FSCV $E_{P,Bkg}$ shifted accordingly when using a conventional two-electrode configuration (Figure 8A). This resulted in loss of dopamine sensitivity, defined as the calibration curve slope (Figure 8B,E). With the three-electrode configuration, accuracy in the applied potential was guaranteed (i.e., no $E_{P,Bkg}$ shift), even with increasing charge-transfer resistance (Figure 8C). Because dopamine identification and quantification are predicated upon accurate cyclic voltammogram potentials, dopamine sensitivity was preserved (Figure 8D,E). The results of this in vitro experiment provided evidence that the three-electrode configuration was capable of compensating for increased electrochemical impedance and preserving dopamine sensitivity.

The two- and three-electrode configurations were also compared in vivo. The $E_{P,Bkg}$ shift was determined for both configurations over 3 weeks of implantation. Because a three-electrode configuration is suited to compensate for increased electrochemical impedance but not reference electrode polarization, the polarization magnitudes of the Ag/AgCl-wire reference electrodes (see Figure 5A) were subtracted from the corresponding total $E_{P,Bkg}$ shifts. This allowed for visualization of the $E_{P,Bkg}$ shift due solely to the electrochemical impedance component of biofouling. We found that the three-electrode configuration successfully compensated for biofouling-induced electrochemical impedance, yielding significantly reduced $E_{P,Bkg}$ shifts in vivo when compared to a conventional two-electrode configuration (Figure 9).

Future studies will focus on stabilization of the reference electrode potential. A stable reference electrode combined with the three-electrode configuration should prevent the chronic $E_{P,Bkg}$ shift, allowing for maximum selectivity and sensitivity to dopamine and confidence in long-term measurement of dopamine in vivo.

CONCLUSIONS

Preserving voltammetric performance and signal fidelity is crucial in long-term in vivo electrochemical studies. Biofouling is a pervasive issue that makes electrochemical measurements increasingly challenging with prolonged electrode implantation in the brain. In long-term dopaminergic FSCV studies, the $E_{P,Bkg}$ shift that occurs days after implantation reduces selectivity and sensitivity to dopamine, complicating quantification. We found that this shift can be attributed to two factors, both likely caused by immune response-induced

encapsulation of the electrodes. One factor, an increase in electrochemical impedance of both the working and reference electrodes, was mitigated with a three-electrode configuration utilizing a Pt-wire counter electrode. The other factor, cathodic polarization of the reference electrode, will be the focus of future studies. Stabilization of the reference electrode potential may involve the use of coatings (e.g., Nafion[25]) or a different reference electrode material altogether. In addition to the instability of Ag/AgCl-wire reference electrodes in vivo, silver toxicity in the brain warrants the use of a more biocompatible reference electrode material. Such a reference electrode, in conjunction with the three-electrode configuration, should provide a permanently stable FSCV background signal that will allow for reliable dopamine detection over the course of weeks to months or longer, improving the validity of long-term dopaminergic signaling research.

Supplementary Material

Refer to Web version on PubMed Central for supplementary material.

ACKNOWLEDGMENTS

All SEM/EDX data were collected in the W. M. Keck Center for Nanoscale Imaging in the Department of Chemistry and Biochemistry at the University of Arizona with funding from the W. M. Keck Foundation Grant. The authors thank James Siegenthaler and Dr. Brooke Massani for their advice and assistance with SEM/EDX. Printed circuit boards for the FSCV headstages were fabricated by H Tech Engineering (Tucson, AZ).

REFERENCES

(1). Bernheimer H; Birkmayer W; Hornykiewicz O; Jellinger K; Seitelberger FJ. Neurol. Sci 1973, 20 (4), 415–455. [PubMed: 4272516]

(2). Wood PB Med. Hypotheses 2004, 62 (3), 420–424. [PubMed: 14975515]

(3). Finan PH; Smith MT Sleep Med. Rev 2013, 17 (3), 173–183. [PubMed: 22748562]

(4). Brown AS; Gershon SJ Neural Transm. 1993, 91 (2–3), 75–109.

(5). Segman RH; Cooper-Kazaz R; Macciardi F; Goltser T; Halfon Y; Dobroborski T; Shalev AY Mol. Psychiatry 2002, 7 (8), 903–907. [PubMed: 12232785]

(6). Stamford JA; Kruk ZL; Millar J; Wightman RM Neurosci. Lett 1984, 51 (1), 133–138. [PubMed: 6334821]

(7). Baur JE; Kristensen EW; May LJ; Wiedemann DJ; Wightman RM Anal. Chem 1988, 60 (13), 1268–1272. [PubMed: 3213946]

(8). Millar J; Stamford JA; Kruk ZL; Wightman RM Eur. J. Pharmacol 1985, 109 (3), 341–348. [PubMed: 3872803]

(9). Roberts JG; Sombers LA Anal. Chem 2018, 90 (1), 490–504. [PubMed: 29182309]

(10). Rodeberg NT; Sandberg SG; Johnson JA; Phillips PEM; Wightman RM ACS Chem. Neurosci 2017, 8 (2), 221–234. [PubMed: 28127962]

(11). Kuhlmann J; Dzugan LC; Heineman WR Electroanalysis 2012, 24 (8), 1732–1738.

(12). Wisniewski N; Moussy F; Reichert WM Fresenius' J. Anal. Chem 2000, 366 (6–7), 611–621. [PubMed: 11225773]

(13). Szarowski DH; Andersen MD; Retterer S; Spence AJ; Isaacson M; Craighead HG; Turner JN; Shain W Brain Res. 2003, 983 (1–2), 23–35. [PubMed: 12914963]

(14). Griffith RW; Humphrey DR Neurosci. Lett 2006, 406 (1–2), 81–86. [PubMed: 16905255]

(15). Roitbak T; Syková E Glia 1999, 28 (1), 40–48. [PubMed: 10498821]

(16). Salatino JW; Ludwig KA; Kozai TDY; Purcell EK Nat. Biomed. Eng 2017, 1 (11), 862–877. [PubMed: 30505625]

(17). Polikov VS; Tresco PA; Reichert WM J. Neurosci. Methods 2005, 148 (1), 1–18. [PubMed: 16198003]

(18). Campbell A; Wu C Micromachines. 2018, 9 (9), 430.

(19). Roberts JG; Lugo-Morales LZ; Loziuk PL; Sombers LA Methods Mol. Biol 2013, 964, 275–294. [PubMed: 23296789]

(20). Heien MLAV; Khan AS; Ariansen JL; Cheer JF; Phillips PEM; Wassum KM; Wightman RM Proc. Natl. Acad. Sci. U. S. A 2005, 102 (29), 10023–10028. [PubMed: 16006505]

(21). Clark JJ; Sandberg SG; Wanat MJ; Gan JO; Horne EA; Hart AS; Akers CA; Parker JG; Willuhn I; Martinez V; Evans SB; Stella N; Phillips PE Nat. Methods 2010, 7 (2), 126–129. [PubMed: 20037591]

(22). Saddoris MP; Wang X; Sugam JA; Carelli RM J. Neurosci 2016, 36 (1), 235–250. [PubMed: 26740664]

(23). Saddoris MP; Cacciapaglia F; Wightman RM; Carelli RM J. Neurosci 2015, 35 (33), 11572–11582. [PubMed: 26290234]

(24). Rodeberg NT; Johnson JA; Bucher ES; Wightman RM ACS Chem. Neurosci 2016, 7 (11), 1508–1518. [PubMed: 27548680]

(25). Hashemi P; Walsh PL; Guillot TS; Gras-Najjar J; Takmakov P; Crews FT; Wightman RM ACS Chem. Neurosci 2011, 2 (11), 658–666. [PubMed: 22125666]

(26). Vreeland RF; Atcherley CW; Russell WS; Xie JY; Lu D; Laude ND; Porreca F; Heien ML Anal. Chem 2015, 87 (5), 2600–2607. [PubMed: 25692657]

(27). Liu X; Xiao T; Wu F; Shen M-Y; Zhang M; Yu H; Mao L Angew. Chem., Int. Ed 2017, 56 (39), 11802–11806.

(28). Shen M; Colombo ML Anal. Methods 2015, 7 (17), 7095–7105. [PubMed: 26327927]

(29). Puthongkham P; Venton BJ ACS Sensors 2019, 4 (9), 2403–2411. [PubMed: 31387349]

(30). Moussy F; Harrison DJ Anal. Chem 1994, 66 (5), 674–679. [PubMed: 8154589]

(31). Bard AJ; Faulkner LR Electrochemical Methods: Fundamentals and Applications, 2nd ed.; Wiley: New York, 2001.

(32). Treseder RS NACE Corrosion Engineer's Reference Book, 2nd ed.; NACE International: Houston, 1991.

(33). Wang B; Yang P; Ding Y; Qi H; Gao Q; Zhang C ACS Appl. Mater. Interfaces 2019, 11 (9), 8807–8817. [PubMed: 30741520]

(34). Lempka SF; Miocinovic S; Johnson MD; Vitek JL; McIntyre CC J. Neural Eng 2009, 6 (4), 046001. [PubMed: 19494421]

(35). Williams JC; Hippensteel JA; Dilgen J; Shain W; Kipke DR J. Neural Eng 2007, 4 (4), 410–423. [PubMed: 18057508]

(36). Mercanzini A; Colin P; Bensadoun J-C; Bertsch A; Renaud P IEEE Trans. Biomed. Eng 2009, 56 (7), 1909–1918. [PubMed: 19362904]

(37). Grill WM; Thomas Mortimer, J. Ann. Biomed. Eng 1994, 22 (1), 23–33.

(38). Weiland JD; Anderson DJ IEEE Trans. Biomed. Eng 2000, 47 (7), 911–918. [PubMed: 10916262]

(39). Randviir EP; Banks CE Anal. Methods 2013, 5 (5), 1098.

(40). Roberts JG; Toups JV; Eyualem E; McCarty GS; Sombers LA Anal. Chem 2013, 85 (23), 11568–11575. [PubMed: 24224460]

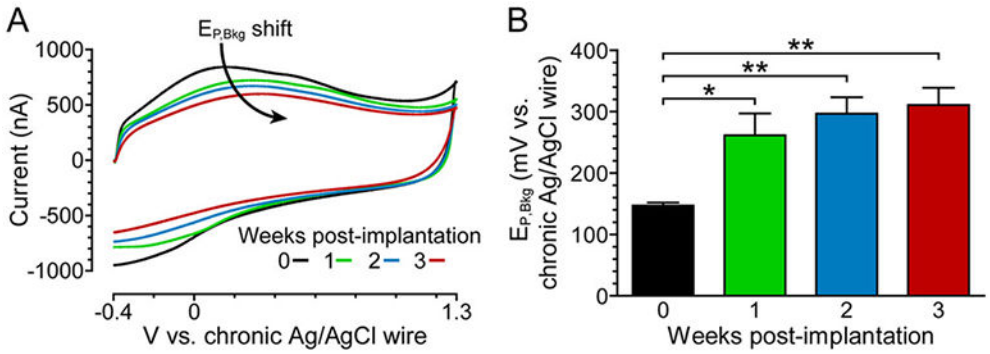

Figure 1.

Peak oxidative potential of the FSCV background signal ($E_{P,Bkg}$) shifts over time in vivo. (A) Representative in vivo FSCV background signals in one-week recording intervals using a conventional two-electrode configuration. (B) Weekly $E_{P,Bkg}$ trend. Mean ± SEM; $n = 4$ rats. A one-way repeated measures ANOVA showed a significant difference in $E_{P,Bkg}$ over time ($F_{3,9} = 13.80$, $p = 0.0010$). Bonferroni posthoc tests: *$p < 0.05$, **$p < 0.01$.

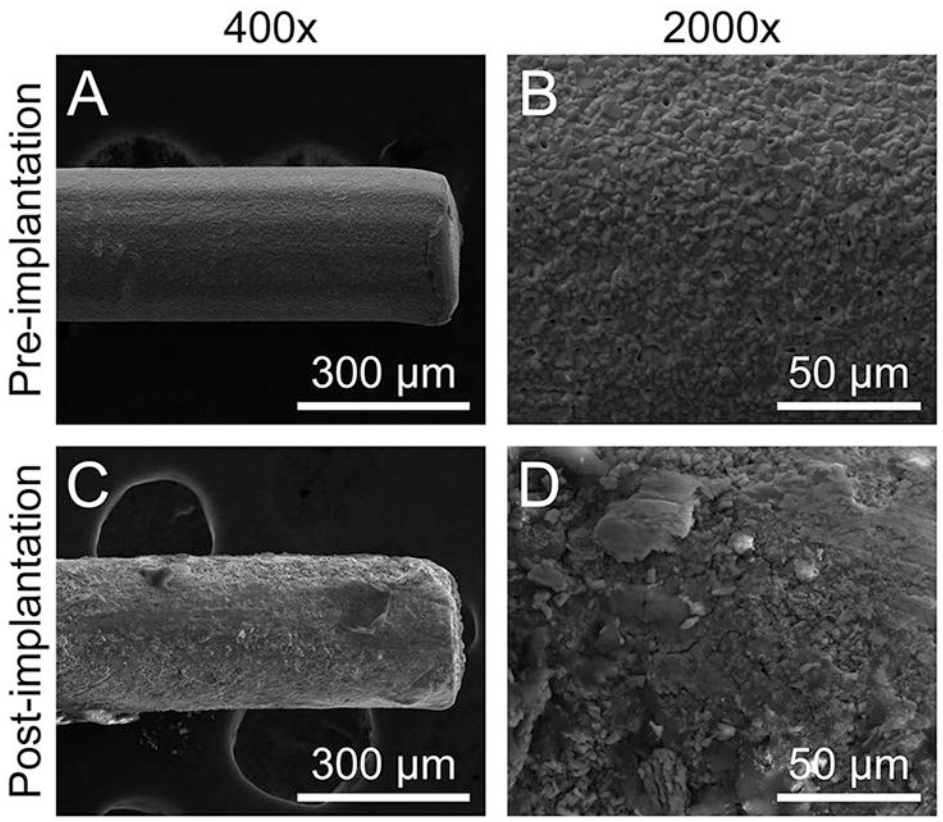

Figure 2.

Ag/AgCl-wire reference electrodes undergo surface-level changes during prolonged brain implantation. (A) 400× and (B) 2000× representative scanning electron micrographs of Ag/AgCl-wire reference electrodes before implantation and (C) 400× and (D) 2000× 3 weeks post-implantation.

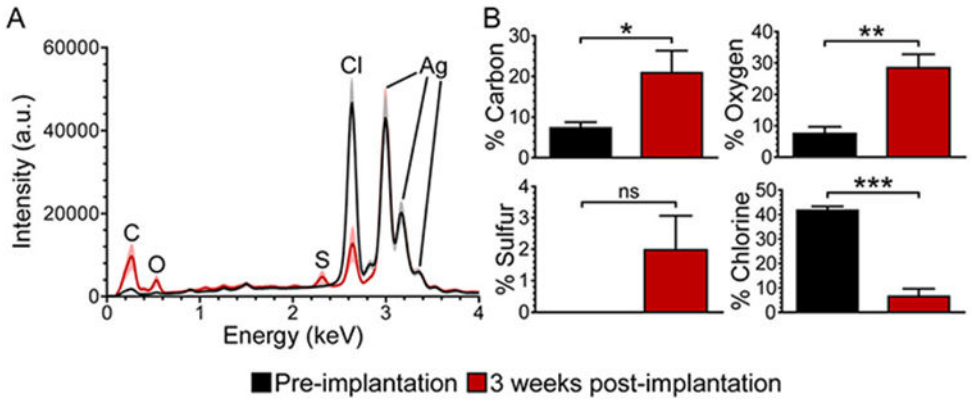

Figure 3.

Surface chlorine decreases, while surface carbon and oxygen increase, on Ag/AgCl-wire reference electrodes during prolonged brain implantation. (A) Averaged EDX spectra for Ag/AgCl-wire reference electrodes preimplantation (black) and 3 weeks post-implantation (red). Line and shading represent mean and SEM, respectively; $n = 6$ rats. (B) EDX percent atomic species for Ag/AgCl-wire reference electrodes, pre- and post-implantation. Mean ± SEM; $n = 6$ rats. Two-tailed paired t test: *$p < 0.05$, **$p < 0.01$, ***$p < 0.001$. There was no significant change in percent atomic silver ($p > 0.05$, not shown in B).

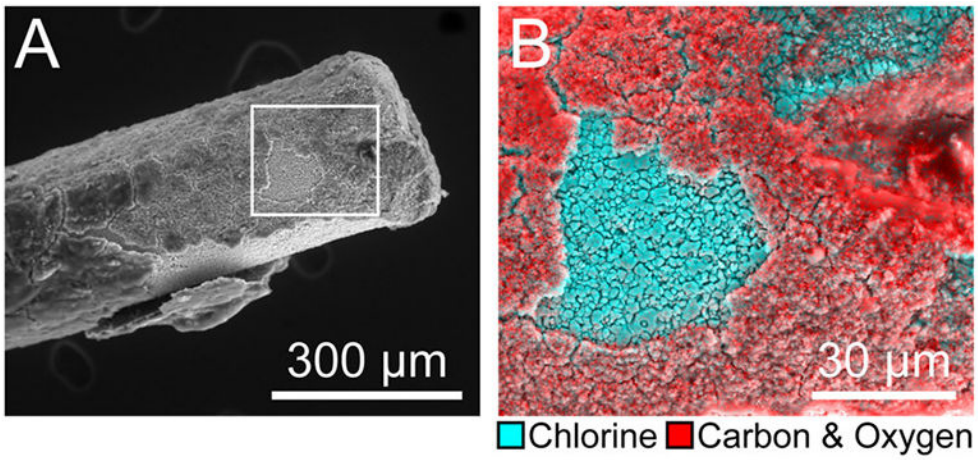

Figure 4.

Prolonged brain implantation induces the formation of an organic sheath around the Ag/AgCl-wire reference electrode. (A) 400× scanning electron micrograph of Ag/AgCl-wire reference electrode 3 weeks post-implantation. (B) 1500× box from A; EDX spectral mapping overlay: cyan = chlorine, red = carbon and oxygen.

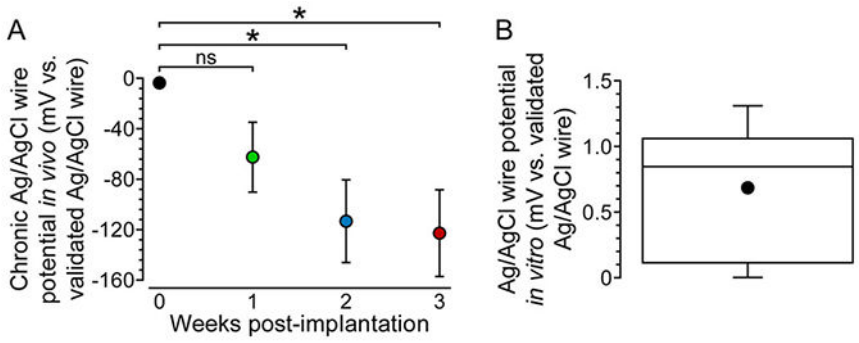

Figure 5.

Prolonged brain implantation causes cathodic polarization of the Ag/AgCl-wire reference electrode. (A) Open circuit potential measurements for chronically implanted Ag/AgCl-wire reference electrodes vs acutely implanted, validated Ag/AgCl-wire reference electrodes in vivo. Mean ± SEM; $n = 4$ rats. A one-way repeated measures ANOVA showed a significant difference in the reference electrode potential over time ($F_{3,9} = 6.472$, $p = 0.0126$). Bonferroni posthoc tests: $*p < 0.05$. (B) Min-to-max box-and-whisker plot showing Ag/AgCl-wire reference electrode potential variability in vitro (aCSF) vs validated Ag/AgCl wire; $n = 15$ electrodes. Dot indicates mean.

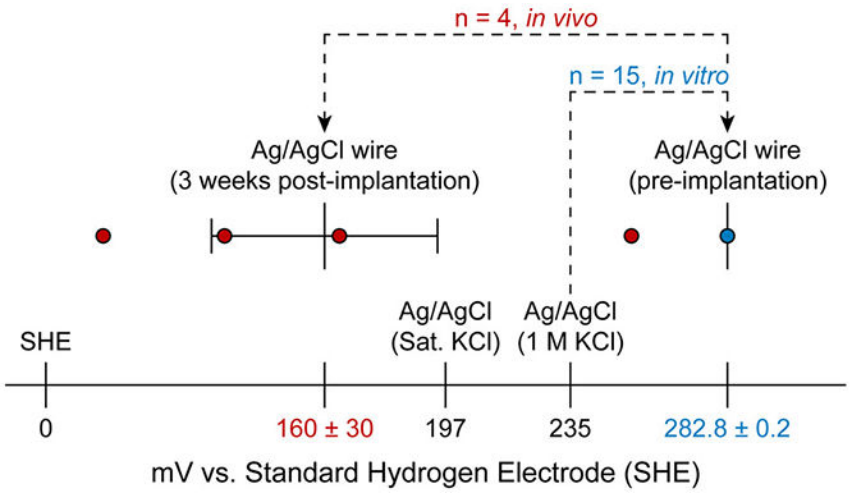

Figure 6.

Variance in the potential of Ag/AgCl-wire reference electrodes increases after 3 weeks of brain implantation. Recorded Ag/AgCl-wire reference electrode open circuit potentials preimplantation (in vitro (aCSF), blue) and 3 weeks post-implantation (in vivo, red). Mean ± SEM for experimental data shown on graph, with numerical values below. Literature values (black) for Ag/AgCl (sat. KCl) and Ag/AgCl (1 M KCl) were obtained from refs 31 and 32, respectively. An *F* test showed a significant difference in Ag/AgCl-wire reference electrode potential variance when comparing in vitro and in vivo recordings ($F_{3,14}$ = 13672, p < 0.0001).

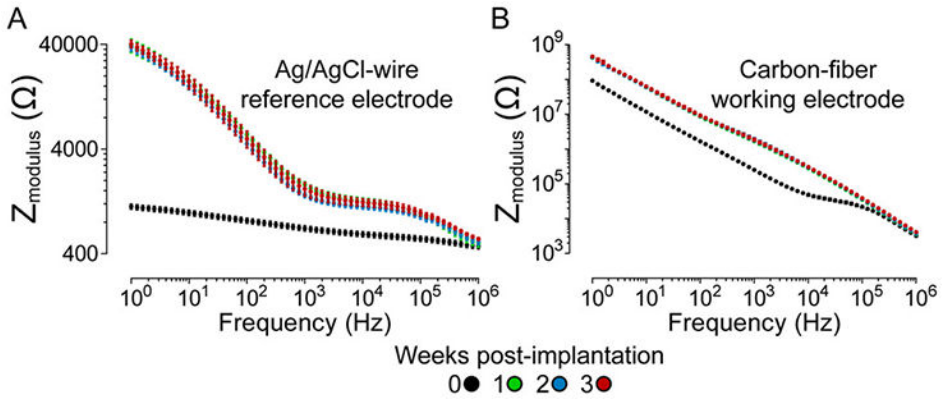

Figure 7.

Prolonged brain implantation increases electrochemical impedance of both the Ag/AgCl-wire and carbon-fiber electrodes, specifically in the charge-transfer resistance frequency regime. EIS Bode plots for chronically implanted (A) Ag/AgCl-wire reference electrodes and (B) carbon-fiber working electrodes. Mean ± SEM; $n = 3$ rats.

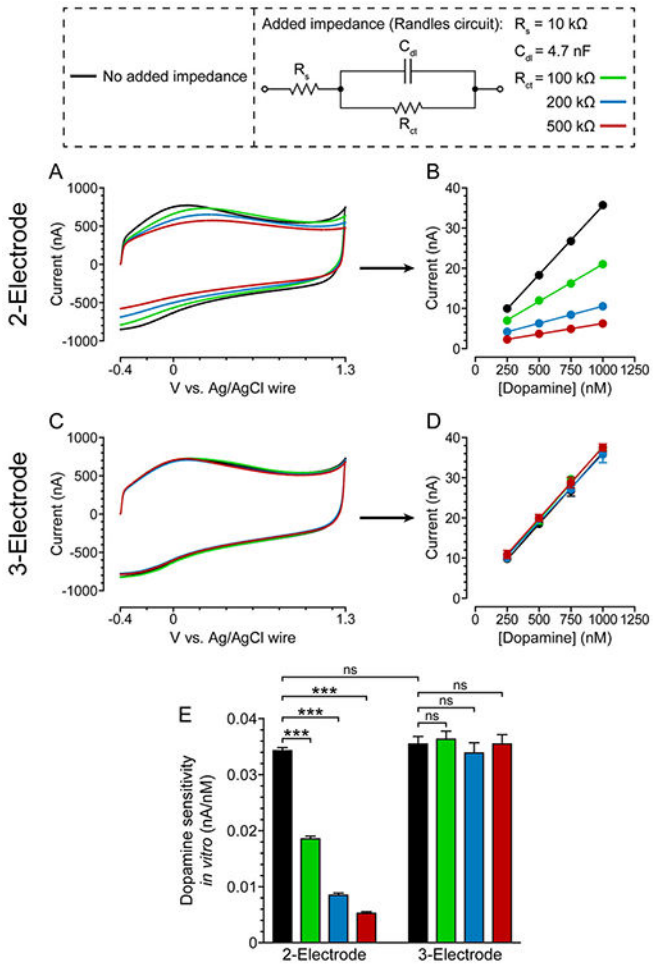

Figure 8.

Three-electrode configuration compensates for increased electrochemical impedance and preserves dopamine sensitivity in vitro (aCSF). (A) Representative two-electrode FSCV background signals in response to increasing charge-transfer resistance in vitro and (B) resultant dopamine calibration curves. Mean ± SEM; $n = 3$ dopamine measurements. Error bars not visible. $R^2 > 0.99$ for all curves. (C) Representative three-electrode FSCV background signals in response to increasing charge-transfer resistance in vitro and (D) resultant dopamine calibration curves. Mean ± SEM; $n = 3$ dopamine measurements. $R^2 > 0.99$ for all curves. (E) Dopamine sensitivity, defined as calibration curve slope, using two- and three-electrode configurations with increasing charge-transfer resistance. Mean ± SEM; $n = 3$ slopes. A two-way ANOVA showed a significant difference in dopamine sensitivity between the two- and three-electrode configurations when comparing added charge-transfer resistance ($F_{1,8} = 510.4$, $p < 0.0001$). Bonferroni posthoc tests: ***$p < 0.001$.

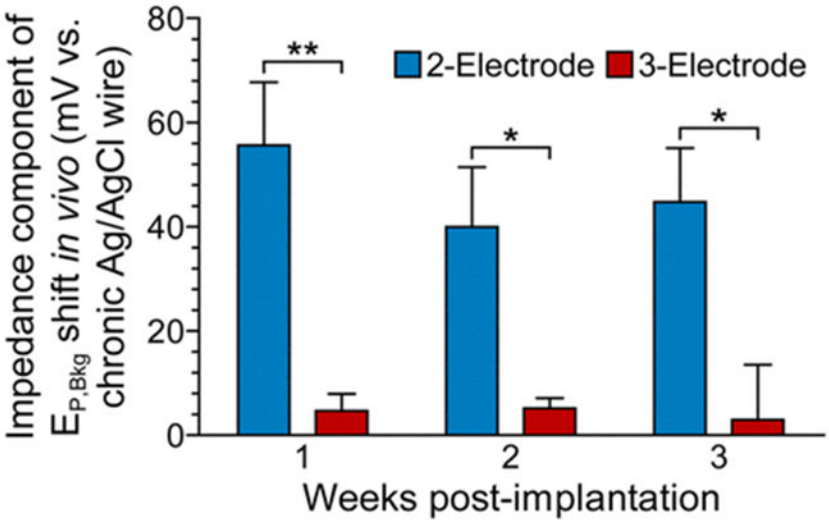

Figure 9.

Three-electrode configuration mitigates biofouling-induced impedance and reduces the FSCV $E_{P,Bkg}$ shift in vivo. $E_{P,Bkg}$ shift, with Ag/AgCl-wire reference electrode polarization component removed, for two- and three-electrode configurations over the course of three-week in vivo implantation. Mean ± SEM; $n = 4$ rats. A two-way repeated measures ANOVA showed a significant difference in the impedance component of the $E_{P,Bkg}$ shift between two- and three-electrode configurations ($F_{1,12} = 29.04$, $p = 0.0017$). Bonferroni posthoc tests: *$p < 0.05$, **$p < 0.01$.